



LAWRENCE
LIVERMORE
NATIONAL
LABORATORY

OPTICAL PROPERTIES OF A MECHANICALLY POLISHED AND AIR-EQUILIBRATED [111] UO₂ SURFACE BY RAMAN AND ELLIPSOMETRIC SPECTROSCOPY

W. J. Siekhaus, J. C. Crowhurst

July 28, 2009

Actinides 2009

San Francisco, CA, United States

July 12, 2009 through July 18, 2009

Disclaimer

This document was prepared as an account of work sponsored by an agency of the United States government. Neither the United States government nor Lawrence Livermore National Security, LLC, nor any of their employees makes any warranty, expressed or implied, or assumes any legal liability or responsibility for the accuracy, completeness, or usefulness of any information, apparatus, product, or process disclosed, or represents that its use would not infringe privately owned rights. Reference herein to any specific commercial product, process, or service by trade name, trademark, manufacturer, or otherwise does not necessarily constitute or imply its endorsement, recommendation, or favoring by the United States government or Lawrence Livermore National Security, LLC. The views and opinions of authors expressed herein do not necessarily state or reflect those of the United States government or Lawrence Livermore National Security, LLC, and shall not be used for advertising or product endorsement purposes.

Optical properties of a mechanically polished and air-equilibrated [111] UO₂ surface by Raman and ellipsometric spectroscopy.

W Siekhaus, J Crowhurst

Lawrence Livermore National Laboratory,
Condensed Matter and Materials Division
Livermore, CA 94550

Siekhaus1@LLNL.Gov

Abstract. Optical constants of a [111] UO₂ surface, aged in air, were measured in the range from .8 and 5 eV using ellipsometric spectroscopy. The ellipsometric data acquired at angles of incidence of 65, 70 and 75 degrees have been fitted by two techniques: 1) First at low energies with a Cauchy-Urbach model extended by the point by point method to higher energies and shown to be Kramers-Kronig consistent, 2) by a Gauss-Lorentz and a Tauc Lorentz Oscillator. Both techniques lead to dielectric constants that differ at energies above 2 eV substantially from Schoenes' for vacuum-annealed [111] UO₂. Raman spectra taken at 632 nm show no indication of hyper-stoichiometry.

1. Introduction

Properties of uranium oxide are of interest in all areas of the nuclear industry. The optical properties of vacuum-annealed signal crystal UO₂ have been determined from near-normal reflectance spectroscopy data by Schoenes [1], [2] [3] and compared to the electronic structure of UO₂. UO₂ encountered in practical situations has been exposed to air. Here we analyze a UO₂ single crystal that has been exposed to air for 25.5 years. R. Schulze of Los Alamos National Laboratory has provided the crystal.

2. Experimental Procedure

The sample was mechanically polished in 1983 and has been exposed since then to laboratory air. It was analyzed in air using a WVASE ellipsometric Spectrometer equipped with a 75-watt light source and a HS-190 monochromator [4]. Ellipsometric data Δ and Ψ were collected at 65°, 70°, and 75° angle of incidence at photon energies between .75 and 5.5 eV. Several runs were performed with and without source-beam collimator (producing different sizes of incident beams) and different iris openings of the detector. The results were indistinguishable. The data were modeled by two techniques: 1) by a Cauchy model with Urbach extension in the low energy range below 2 eV, extended to higher energies by the point by point method and checked thereafter for Kramers-Kronig consistency. In the Cauchy model the index of refraction n and the extinction coefficient k are given

$$\text{by } n(\lambda) = A + \frac{B}{\lambda^2} + \frac{C}{\lambda^3} + \dots, \quad k(\lambda) = \text{Amp}_k e^{\text{Exponent}_k * (E - E_k)}, \quad E = \frac{1240}{\lambda}, \quad (1)$$

2) by fitting two oscillators, a Gauss-Lorentz for the low-energy and a Tauc-Lorentz Oscillator for the high-energy range directly to the data. A Gaussian oscillator has the form

$$\varepsilon_2(E) = \text{Amp} \left(e^{-\left(\frac{E-E_n}{\sigma}\right)^2} - e^{-\left(\frac{E+E_n}{\sigma}\right)^2} \right), \quad \sigma = \frac{\text{Br}}{2\sqrt{\ln(2)}} \quad (2)$$

Fit parameters are the amplitude (*Amp*), the center energy (E_n) and the broadening (*Br*) of the absorption peak. *Br* equals the Full-Width-Half-Maximum (FWHM) value. Gauss-Lorentz and Tauc-Lorentz oscillators have additional parameters. The quality of the fit is describe by

$$\text{MSE} = \sqrt{\frac{1}{2N - M} \sum_{n=1}^N \left[\left(\frac{\Psi_i^{\text{mod}} - \Psi_i^{\text{exp}}}{\sigma_{\Psi,i}^{\text{exp}}} \right)^2 + \left(\frac{\Delta_i^{\text{mod}} - \Delta_i^{\text{exp}}}{\sigma_{\Delta,i}^{\text{exp}}} \right)^2 \right]}, \quad M = \text{Number of parameters} \quad (3)$$

Raman spectroscopy using 632nm light was performed at low and high resolution to check the oxidation state of the sample.

3. Experimental Results

The Raman spectrum (see figure 2) showed no indication of hyperstoichiometry. The Cauchy-Urbach fit produced the parameters $A_n=2.2715$, $B_n=1.1993$, $C_n=.055061$, $\text{Amp}_k=1.7835$, $\text{Exponent}_k=1.3794$ and an excellent MSE value of 1.092. (See equations 1 and 3). The Tauc-Lorentz oscillator had the parameters: $\text{Amp}_1=130.8$, $C_1=2.1538$, $E_{\text{offset}}=1.8572$, $E_n1=3.5646$, $E_g1=2.7289$, and the Gauss-Lorentz oscillator had the parameters: $\text{Amp}_2=2.2015$, $E_n2=2/4467$, $\text{PoleMag}_0=.45405$, $\text{Br}_2=1.7716$, $\text{PolePos}_0=5.8396$, $\text{PoleMag}_2=.010032$, $\text{Pole Pos}_2=.70399$. The MSE value of the oscillator fit was 5.238, a value considered to be indicative of a good fit. The different types of fit produced indistinguishable results. Figure 3 shows our dielectric constants ε_1 and ε_2 together with those of Schoenes, and figure 4 the optical constants n and k as a function of energy or wavelength. Table 1 lists the dielectric constants ε_1 and ε_2 as a function of energy.

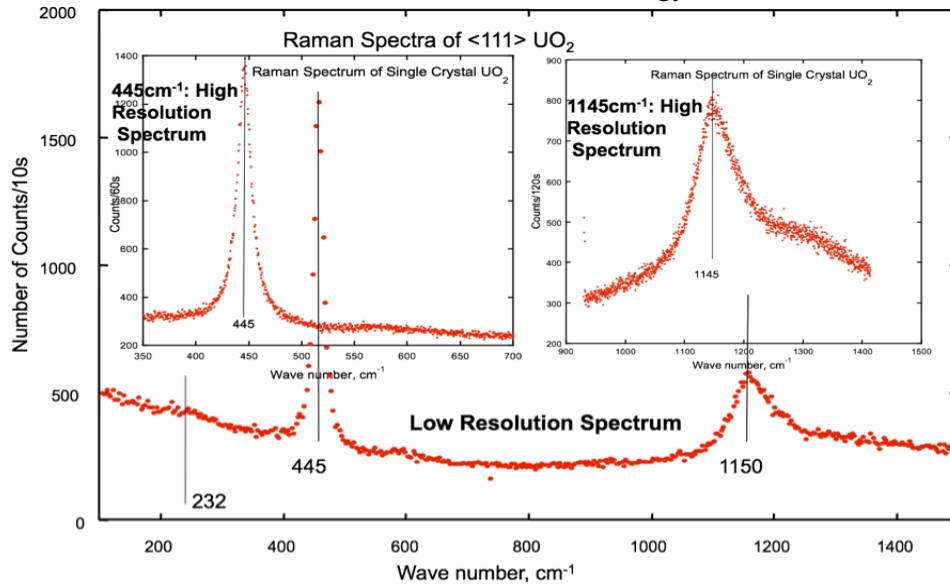


Figure 2. The Raman spectrum taken at high and low resolution using 632 nm laser light.

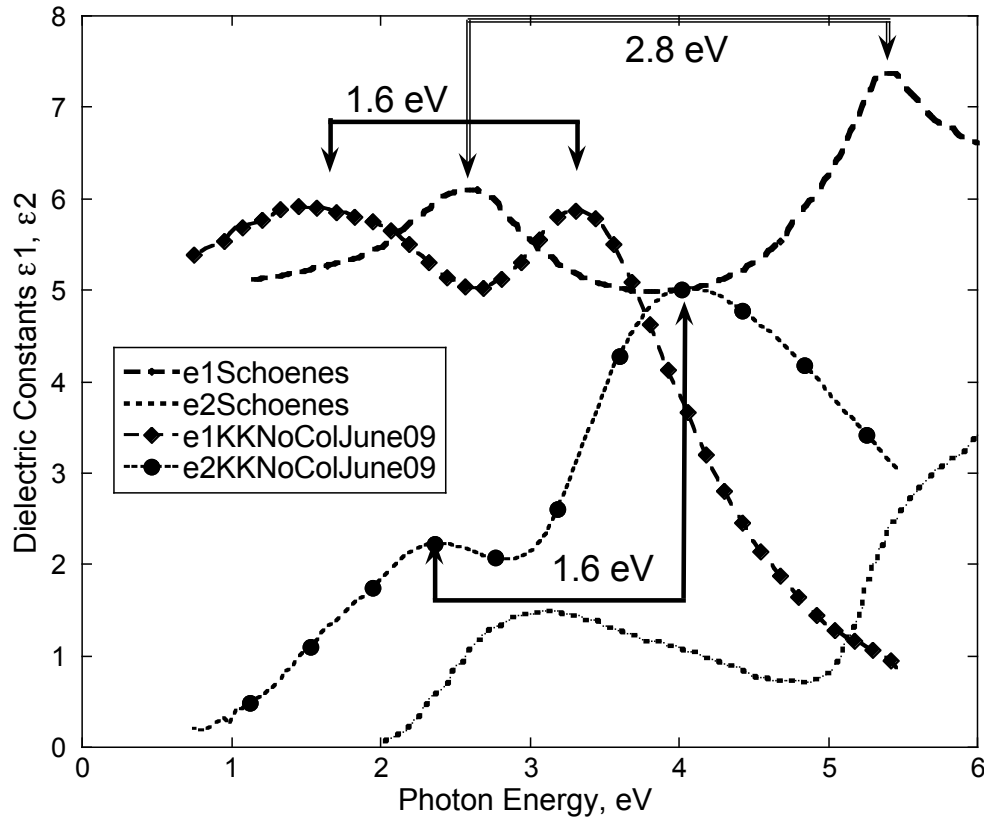


Figure 3. Comparison of our results derived from spectroscopic ellipsometry with Schoenes' results derived from near-normal reflectance data.

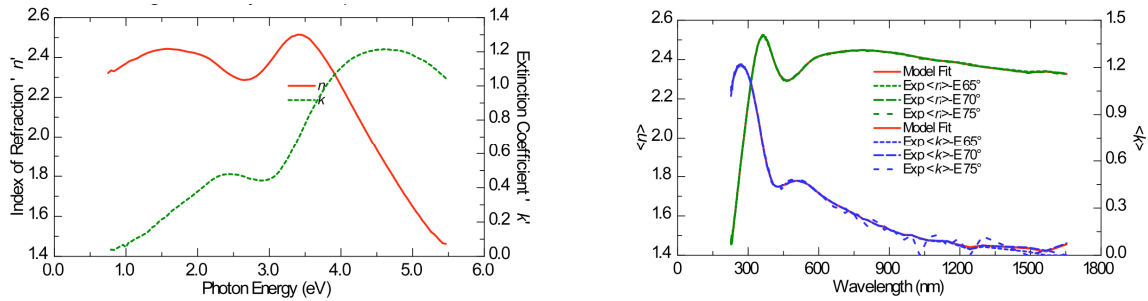


Figure 4. The optical constants n and k as a function of energy or wavelength.

Table 1. The dielectric constants ϵ_1 and ϵ_2 of $[111]$ UO_2 exposed to air for 25.5 years

eV	ϵ_1	ϵ_2	eV	ϵ_1	ϵ_2	eV	ϵ_1	ϵ_2
5.462	0.8978	3.089	3.891	4.341	4.936	2.362	5.274	2.201
5.421	0.9759	3.130	3.850	4.509	4.878	2.321	5.334	2.194
5.379	1.040	3.175	3.809	4.665	4.802	2.279	5.401	2.172
5.338	1.035	3.211	3.767	4.819	4.730	2.238	5.465	2.141
5.297	1.042	3.338	3.726	4.979	4.641	2.197	5.531	2.101
5.255	1.076	3.406	3.685	5.121	4.522	2.155	5.590	2.041
5.214	1.113	3.496	3.643	5.271	4.444	2.114	5.638	1.979
5.173	1.144	3.579	3.602	5.425	4.292	2.073	5.679	1.919
5.131	1.202	3.684	3.561	5.552	4.147	2.031	5.713	1.851

5.090	1.259	3.709	3.519	5.674	3.982	1.990	5.743	1.789
5.049	1.280	3.794	3.478	5.765	3.794	1.949	5.768	1.727
5.007	1.317	3.869	3.437	5.835	3.621	1.907	5.790	1.665
4.966	1.363	3.961	3.395	5.893	3.432	1.866	5.808	1.604
4.925	1.421	4.036	3.354	5.907	3.223	1.825	5.828	1.547
4.883	1.498	4.147	3.313	5.915	3.088	1.783	5.844	1.490
4.842	1.577	4.179	3.271	5.913	2.883	1.742	5.869	1.441
4.801	1.631	4.255	3.230	5.872	2.731	1.701	5.896	1.368
4.759	1.711	4.334	3.189	5.833	2.594	1.659	5.909	1.296
4.718	1.793	4.403	3.147	5.781	2.447	1.618	5.932	1.244
4.677	1.881	4.472	3.106	5.708	2.322	1.577	5.937	1.136
4.635	1.980	4.536	3.065	5.619	2.208	1.535	5.934	1.093
4.594	2.082	4.580	3.023	5.519	2.137	1.494	5.946	1.007
4.553	2.173	4.630	2.982	5.428	2.088	1.453	5.928	0.9237
4.511	2.262	4.676	2.941	5.347	2.058	1.411	5.927	0.8839
4.470	2.366	4.743	2.899	5.277	2.036	1.370	5.928	0.7797
4.429	2.480	4.789	2.858	5.213	2.033	1.329	5.896	0.7028
4.387	2.587	4.829	2.817	5.160	2.035	1.287	5.847	0.6281
4.346	2.706	4.885	2.775	5.125	2.053	1.246	5.826	0.6198
4.305	2.834	4.911	2.734	5.097	2.051	1.205	5.817	0.5227
4.263	2.959	4.957	2.693	5.070	2.078	1.163	5.760	0.4603
4.222	3.100	4.987	2.651	5.059	2.096	1.122	5.714	0.4408
4.181	3.239	4.998	2.610	5.060	2.127	1.081	5.711	0.4201
4.139	3.383	5.018	2.569	5.075	2.151	1.039	5.695	0.3206
4.098	3.528	5.023	2.527	5.098	2.170	0.9980	5.602	0.2437
4.057	3.678	5.030	2.486	5.129	2.188	0.9567	5.540	0.2927
4.015	3.836	5.025	2.445	5.173	2.202	0.8327	5.504	0.2087
3.974	3.999	5.005	2.403	5.223	2.204	0.7913	5.419	0.1144
3.933	4.186	4.990				0.7500	5.349	0.3251

4. Discussion

Our data represent correctly represent the optical properties to be expected from air-exposed uranium oxide. There is clearly a substantial difference between our and Schoenes' data. One possible reason (mentioned by Schoenes in reference [1]) is the fact that the reflectance is strongly affected by the perfection of the surface. Ellipsometry is on the other hand is not strongly affected. Another possible reason could be the formation of a hyperstoichiometric layer on the surface of our sample – even though our Raman spectrum indicates that our sample is stoichiometric UO_2 . Manara [5] determined Raman spectra of stoichiometric and hyperstoichiometric UO_2 using 514 nm light and observed – albeit at much lower resolution than shown in figure 2 - a detectable up-shift in the peak at 445 cm^{-1} only for hyperstoichiometry above $\text{UO}_{2.05}$. No such shift is detectable in figure 3; hence it is important to determine whether Raman spectroscopy at 632nm and ellipsometry analyze the same region of the sample, and to calculate the depth of the layer that may have become hyperstoichiometric due to exposure to air.

Exposing UO_2 to air at low temperature results in a two-step reaction: $\text{UO}_2 \rightarrow \text{U}_4\text{O}_9 / \text{U}_3\text{O}_7 \rightarrow \text{U}_3\text{O}_8$ with U_3O_7 being preferentially formed on un-irradiated UO_2 . The oxidation is controlled by the diffusion of oxygen through the U_3O_7 layer, and the parabolic kinetic data are thus typically fitted to an equation of the form

$$\tau = \sqrt{kt}, \text{ with } \tau = \text{U}_3\text{O}_7 \text{ layer thickness, cm; } k, \text{ m}^2/\text{s; } t = \text{time, s} \quad (4)$$

Kinetic data have been acquired since 1957 [6], and critically evaluated in recent reviews [7] [8] [9] resulting in $k=2.014 \cdot 10^{-7} \cdot \exp[-12534/T]$ [8]. That equation predicts an U_3O_7 ($=\text{UO}_{2.33}$) layer thickness of 6.5 nm after 25.5 years of air exposure at 20°C. Using our optical constants in figure 4 one can determine the average depth $\langle x \rangle$ below the surface from which a Raman or ellipsometric

signal originates, and the fraction of the signal that originates from the predicted U_3O_7 layer of ~ 7 nm. Assuming that the angle of incidence from normal to the surface is β ($=0$ for Raman, $\sim 70^\circ$ for ellipsometry), then $\langle x \rangle$ and the fraction of the signal originating from depth less than 7nm are given by equation 5

$$\langle x \rangle = \int_0^\infty x \frac{2\alpha(\lambda)e^{-2\alpha(\lambda)x/\cos\beta}}{\cos\beta}, \lambda = \text{wavelength}, \alpha(\lambda) = \frac{4\pi k}{\lambda}$$

At $\lambda = 632$ nm, $\beta = 0$ (Raman), $k = .3$, $\langle x \rangle = 83.82\text{nm}$

Fraction of the Raman signal from the first 7 nm = 8% for $\lambda = 632$ nm (5)

At $\lambda = 632$ nm, $\beta = 70$ (ellipsometry), $k = .3$, $\langle x \rangle = 28.1\text{nm}$

Fraction of the ellipsometry signal originating from the first 7 nm = 22% for $\lambda = 632$ nm

Allen et al. [10] showed that while U_4O_9 results in up-shift of the peak at 445cm^{-1} , U_3O_7 produces only a small and very broad feature at 445cm^{-1} . Since (see equation 5) only 8% of our Raman signal in figure 2 originates from the 7 nm thick U_3O_7 layer it is likely that the broadening would not be apparent in figure 2. The ellipsometric data, however, may be influenced by the optical properties of the hyperstoichiometric layer, since 22 % of the ellipsometric signal originates from that layer. However, for energies less than 1.35 eV, we determine k to be less than .15, and only 8.2% of the ellipsometric signal originates from the first 7 nm; hence our n and k values below 1.35 eV represent the properties of $\text{UO}_{2.0}$. Schoenes data, in contrast, show ϵ_2 to be zero below 2 eV, implying that $\text{UO}_{2.0}$ is transparent to red (and longer wavelength) light. At energies above 3 eV, our data are clearly be substantially influenced by a 7nm thick U_3O_7 layer. The sample will be re-analyzed after either vacuum annealing at 1700 K, or after grazing-angle ion-ablating 10 nm from the surface.

References

- [1] Schoenes, J. (1978). "Optical-Properties and Electronic-Structure of UO_2 ." *J. Appl. Phys.* **49**(3): 1463-65.
- [2] Schoenes, J. (1980). "Electronic-Transitions, Crystal-Field Effects and Phonons in UO_2 ." *Phys. Rep.-Rev. Sect. Phys. Lett.* **63**(6): 301-36.
- [3] Schoenes, J. (1987). "Recent Spectroscopic Studies of UO_2 ." *J. Chem. Soc., Faraday Trans. 2.* **83**: 1205-1213.
- [4] J. A. Woollam CO. Inc., Lincoln, NE 68508-2243 USA
- [5] Manara, D. and B. Renker (2003). "Raman spectra of stoichiometric and hyperstoichiometric uranium dioxide." *J. Nucl. Mat.* **321**(2-3): 233-37.
- [6] Aronson, S., R. B. Roof, et al. (1957). "Kinetic Study of the Oxidation of Uranium Dioxide." *J. Chem. Phys.* **27**(1): 137-44.
- [7] McEachern, R. J. (1997). "A review of kinetic data on the rate of U_3O_7 formation on UO_2 ." *J. Nucl. Mat.* **245**(2-3): 238-S47.
- [8] McEachern, R. J. and P. Taylor (1998). "A review of the oxidation of uranium dioxide at temperatures below 400 degrees C." *J. Nucl. Mat.* **254**(2-3): 87-121.
- [9] Poulesquen, A., L. Desgranges, et al. (2007). "An improved model to evaluate the oxidation kinetics of uranium dioxide during dry storage." *J. Nucl. Mat.* **362**: 402-10.
- [10] Allen, G. C., I. S. Butler, et al. (1987). "Characterization of Uranium-Oxides by Micro-Raman Spectroscopy." *J. Nucl. Mat.* **144**(1-2): 17-19.

"

"

"

Vj ku'y qtnlr gthqto gf "wpf gt"vj g"cwur legu"qh"vj g"WUOF gr ctwo gpv"qh"Gpgti { "d{ "Ncy tgpeg"Nkxgto qtg"
P cwkqpcnNcdqtcvqt{ "wpf gt"EqpvtcevF G/CE74/29P C495660